

HClO_4 at +0.50 V, from the current-time curve given by $5 \times 10^{-4} M \text{HClO}_2$ in $1 M \text{HClO}_4$ at the same potential. The agreement between experimental and theoretical curves is good. An analogous agreement is encountered in comparing the experimental current-potential characteristics with the corresponding theoretical characteristics as obtained from eq 18. In this connection a series of theoretical voltammograms was calculated for $D = 0.8 \times 10^{-5} \text{ cm}^2/\text{sec}$, $r_0 = 0.094 \text{ cm}$, $t_1 = 5 \text{ sec}$, and for several values of σ . These voltammograms were subsequently corrected for the "washing period," $t_p = 3 \times 10^{-2} \text{ sec}$, by following a procedure described in ref 7. The above values of D , r_0 , t_1 , and t_p correspond to the experimental conditions employed in the measurements. From the comparison between the theoretical voltammograms and the experimental curve of $5 \times 10^{-4} M \text{HClO}_2$ in $1 M \text{HClO}_4$ it has been possible to attribute the value 0.3 to the rate constant σ in $1 M \text{HClO}_4$. The theoretical current-potential characteristic corresponding to this value of σ is repre-

sented by the solid curve in Figure 8, whereas circles express the experimental voltammetric curve.

Unfortunately the uncertainty about the value for the dissociation constant, K , of HClO_2 as well as the error made in the evaluation of the liquid junction potential cause the experimental value for $E(0) - E_{1/2}$ to be inaccurate. It follows that the value of σ is also roughly approximate. Furthermore it must be noted that the value of σ depends upon the state of the surface of the platinized platinum electrode. Thus the voltammetric curves recorded on platinum electrodes platinized some days before recording are characterized by $E(0) - E_{1/2}$ values lower than that obtained with a freshly platinized electrode even by 30 mV, as a consequence of a decrease in σ due to the aging of the platinization.

Acknowledgments. The present work was partially supported by CNR (Consiglio Nazionale delle Ricerche) under Contracts No. 115.1332.0-0469 and 115.-1642.0-4400.

Electronic Spectra of the Dithioacetylacetonate Complexes of Nickel(II), Palladium(II), and Platinum(II)¹

Olavi Siimann and James Fresco

Contribution from the Chemistry Department, McGill University, Montreal, Canada. Received August 18, 1969

Abstract: An extended Wolfsberg-Helmholz molecular orbital calculation has been performed for bis(dithioacetylacetonato)nickel(II). The energy level diagram produced permitted assignment of the electronic spectra of nickel(II), palladium(II), and platinum(II) dithioacetylacetonates recorded in coordinating and noncoordinating solvents. Bands in the electronic spectrum of cobalt(II) dithioacetylacetonate were also assigned. Values obtained for the splitting parameter, Δ_1 , of the nickel(II) and palladium(II) complexes indicated that the dithioacetylacetonate anion assumes an intermediate position in a spectrochemical series of sulfur donors.

The electronic spectra of planar d^8 metal complexes containing sulfur donor atoms have been investigated to establish the properties of the molecular orbitals in planar metal complexes. Semiempirical molecular orbital calculations were performed for metal dithiolates,² dithiooxalates,³ and dithienes.⁴ The recent synthesis of metal complexes of dithioacetylacetonate⁵ in which the donor atoms exist in six-membered rather than five-membered rings has stimulated interest in their spectral properties.^{5a}

The electronic properties of dithioacetylacetonates appear more similar to those of dithiolates than acetylacetonates. The profound influence of sulfur can be further noted in the electronic spectra of monothioacetylacetonates.⁶ These spectra have a greater re-

semblance to the spectra of dithioacetylacetonates than acetylacetonates.

A molecular orbital calculation for the diamagnetic nickel(II) chelate of dithioacetylacetonate has been performed to determine the energies of the molecular orbitals of the complex and to ascertain the donor properties of the dithioacetylacetonate anion. Since the observed absorption bands of the complex could be reasonably assigned and agreement exists between observed and calculated frequencies, the Wolfsberg-Helmholz^{7,8} molecular orbital calculation employed appears satisfactory. The results obtained will be reported here.

Experimental Section

The complexes studied were prepared by previously described methods.^{5b} All spectra were recorded on a Perkin-Elmer 350 spectrophotometer. Matched pairs of quartz cells of 1.0- and 10.0-cm path lengths were used to examine solutions over the concentration range 0.001-0.00001 M . Spectrograde solvents were employed without further purifications.

(1) A preliminary account of this work was presented at the 52nd Canadian Chemical Conference, Montreal, May 1969.

(2) S. I. Shupack, E. Billig, R. J. H. Clark, R. Williams, and H. B. Gray, *J. Amer. Chem. Soc.*, **86**, 4594 (1964).

(3) A. R. Latham, V. C. Hascall, and H. B. Gray, *Inorg. Chem.*, **4**, 788 (1965).

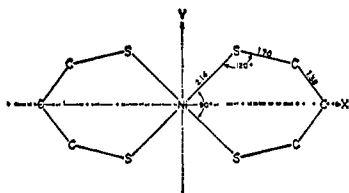
(4) G. N. Schrauzer and V. P. Mayweg, *J. Amer. Chem. Soc.*, **87**, 3585 (1965).

(5) (a) A. Ouchi, M. Hyodo, and Y. Takahashi, *Bull. Chem. Soc. Jap.*, **40**, 2819 (1967); (b) O. Siimann and J. Fresco, *Inorg. Chem.*, **8**, 1846 (1969).

(6) S. H. H. Chaston and S. E. Livingstone, *Aust. J. Chem.*, **20**, 1079 (1967).

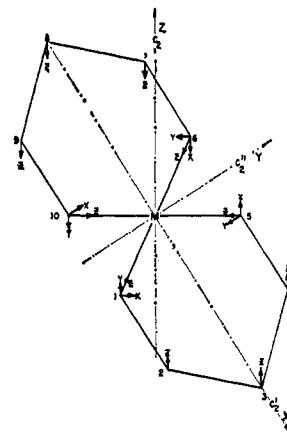
(7) M. Wolfsberg and L. Helmholz, *J. Chem. Phys.*, **20**, 837 (1952).

(8) C. J. Ballhausen and H. B. Gray, *Inorg. Chem.*, **1**, 111 (1962).

Figure 1. Structure of Ni(DTAA)₂.

Method of Calculation

The structure of bis(dithioacetylacetonato)cobalt(II) as shown by X-ray diffraction⁹ possesses D_{2h} point symmetry, if the methyl groups which do not contribute to the π -electron system in the ligands are disregarded. Bond distances and angles estimated for the isostructural bis(dithioacetylacetonato)nickel(II)⁹ are shown in Figure 1. For the purpose of molecular orbital calculations the nickel and sulfur atoms were considered σ - and π -bonded while only π bonding within the ligands was taken into account. In contrast to calculations performed for metal dithiolates,² where a separate computation was initially performed for the ligands alone, it was possible to treat the entire Ni(DTAA)₂ molecule in one calculation. The coordinate system adopted for the 1:2 metal-ligand model is shown in Figure 2. By convention the metal X and Y axes lie between metal-sulfur bonds and the sulfur Z axes point toward the metal. All the nickel 3d, 4s, and 4p orbitals were considered in the calculation. Since the angle between the nickel-sulfur and sulfur-carbon bonds is 120° , the in-plane σ and π sulfur wave functions were constructed as sp^2 hybrids of the 3s and 3p sulfur orbitals. The

Figure 2. Coordinate system for Ni(DTAA)₂.

metal atomic orbitals and symmetry-adapted ligand orbitals in D_{2h} symmetry are given in Table I.

To evaluate the two-center atomic overlap integrals, self-consistent field functions as linear combinations of Slater orbitals were used. The SCF functions of nickel 3d,^{10a} 4s,^{10a} and 4p^{10b} orbitals, sulfur 3s^{10c} and 3p^{10c} orbitals, and the carbon 2p^{10d} orbital were obtained from previous studies. Group overlap integrals, G_{ij} , resulting from overlap of symmetrized orbitals are listed in Table II. Overlaps based on orbitals of principal quantum number four for which Slater overlaps,¹¹ S_{ij} , are not available were interpolated from S_{ij} values for orbitals of quantum numbers three and five.

Table I. Wave Functions for Ni(DTAA)₂

Species	Metal orbital	Ligand orbital
A_g	3d _{z²}	$\phi_1 = \frac{1}{2}(\sigma_1 + \sigma_5 + \sigma_6 + \sigma_{10})$
	3d _{x²-y²}	$\phi_2 = \frac{1}{2}(\sigma_1' + \sigma_5' + \sigma_6' + \sigma_{10}')$
	4s	
B_{1g}	3d _{xy}	$\phi_3 = \frac{1}{2}(\sigma_1 - \sigma_5 + \sigma_6 - \sigma_{10})$
		$\phi_4 = \frac{1}{2}(\sigma_1' - \sigma_5' + \sigma_6' - \sigma_{10}')$
B_{2u}	4p _y	$\phi_5 = \frac{1}{\sqrt{2}}(\sigma_5 - \sigma_{10})$
		$\phi_6 = \frac{1}{\sqrt{2}}(\sigma_1' - \sigma_6')$
B_{3u}	4p _z	$\phi_7 = \frac{1}{\sqrt{2}}(\sigma_1 - \sigma_6)$
		$\phi_8 = \frac{1}{\sqrt{2}}(\sigma_5' - \sigma_{10}')$
A_u		$\phi_9 = \frac{1}{2}(y_1 - x_5 - x_6 + y_{10})$ $\phi_{10} = \frac{1}{2}(z_2 - z_4 - z_7 + z_9)$
B_{1u}	4p _x	$\phi_{11} = \frac{1}{2}(y_1 + x_5 - x_6 - y_{10})$
		$\phi_{12} = \frac{1}{2}(z_2 + z_4 - z_7 - z_9)$
		$\phi_{13} = \frac{1}{\sqrt{2}}(z_3 - z_8)$
B_{2g}	3d _{z²}	$\phi_{14} = \frac{1}{2}(y_1 + x_5 + x_6 + y_{10})$
		$\phi_{15} = \frac{1}{2}(z_2 + z_4 + z_7 + z_9)$
		$\phi_{16} = \frac{1}{\sqrt{2}}(z_3 + z_8)$
B_{3g}	3d _{xy}	$\phi_{17} = \frac{1}{2}(y_1 - x_5 + x_6 - y_{10})$
		$\phi_{18} = \frac{1}{2}(z_2 - z_4 + z_7 - z_9)$

(9) R. Beckett and B. F. Hoskins, *Chem. Commun.*, 909 (1967).

Table II. Group Overlap Integrals

$a_g(\sigma)$	$G(4s, \phi_1)$	0.870
$a_g(\sigma)$	$G(3d, \phi_1)$	0.130
$a_g(\pi)$	$G(3d, \phi_2)$	0.100
$b_{1g}(\sigma)$	$G(3d, \phi_3)$	0.225
$b_{1g}(\pi)$	$G(3d, \phi_4)$	0.100
$b_{2u}(\sigma)$	$G(4p, \phi_5)$	0.790
$b_{2u}(\pi)$	$G(4p, \phi_6)$	0.180
$b_{3u}(\sigma)$	$G(4p, \phi_7)$	0.790
$b_{3u}(\pi)$	$G(4p, \phi_8)$	0.180
$b_{1u}(\pi)$	$G(4p, \phi_{11})$	0.360
$b_{2g}(\pi)$	$G(3d, \phi_{14})$	0.060
$b_{3g}(\pi)$	$G(3d, \phi_{17})$	0.060
$a_u, b_{1u, 2g, 3g}(\pi)$	$G(3p_s, 2p_c)$	0.225
$b_{1u, 2g}(\pi)$	$G(2p_c, 2p_c)$	0.465

The method of calculating diagonal coulomb terms, H_{ii} , has been described previously.¹² Values of coulomb integrals that appear in Table III best reproduce the observed data and achieve self-consistency in metal charge distribution. The expression,¹³ $H_{ij} = (2 - |S_{ij}|)(H_{ii} + H_{jj})G_{ij}/2$, was used to evaluate off-diagonal resonance terms. The charge on each atom was cal-

(10) (a) R. E. Watson, *Phys. Rev.*, **119**, 1934 (1960); (b) J. W. Richardson, R. R. Powell, and W. C. Nieuwpoort, *J. Chem. Phys.*, **38**, 796 (1963); (c) G. L. Malli, *Can. J. Phys.*, **44**, 3121 (1966); (d) E. Clementi, C. C. J. Roothaan, and M. Yoshimine, *Phys. Rev.*, **127**, 1618 (1962).(11) (a) R. S. Mulliken, C. A. Rieke, D. Orloff, and H. Orloff, *J. Chem. Phys.*, **17**, 1248 (1949); (b) H. H. Jaffe and G. O. Doak, *ibid.*, **21**, 196 (1953); (c) H. H. Jaffe, *ibid.*, **21**, 258 (1953); (d) D. P. Craig, A. Maccoll, R. S. Nyholm, L. E. Orgel, and L. E. Sutton, *J. Chem. Soc.*, 354 (1954); (e) J. L. Roberts and H. H. Jaffe, *J. Chem. Phys.*, **27**, 883 (1957).(12) H. Basch, A. Viste, and H. B. Gray, *ibid.*, **44**, 10 (1966).(13) L. C. Cusachs, *ibid.*, **43**, S157 (1965).

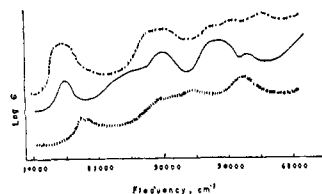


Figure 3. Electronic absorption spectra of dithioacetylacetonates in methanol solution: — · — ·, Pt(DTAA)₂; —, Ni(DTAA)₂; · · · · ·, Pd(DTAA)₂. The value of ϵ corresponds numerically to 1000 cm²/mol.

culated by a Mulliken population analysis¹⁴ and the metal orbital coulomb terms were corrected until the values obtained corresponded to self-consistent metal charge distribution and orbital population as shown in

Table III. Coulomb Integrals and Charge Configurations

Orbital	$-H_{ii}$, 10 ³ cm ⁻¹
σ (S)	120.0
π_h (S)	110.0
π_v (S)	130.0
π_v (C)	89.0
3d (Ni)	101.0
4s (Ni)	74.2
4p (Ni)	40.5
Input	Charge on Ni +0.19
Output	Charge on Ni +0.27
	Ni configuration s ^{0.88} p ^{0.06} d ^{8.88}
	s ^{0.84} p ^{0.06} d ^{8.84}

Table III. The factored secular determinant, $|H_{ij}G_{ij}^{-1} - E\lambda| = 0$, was solved by use of the McGill University IBM 360-75 computer for eigenvalues and eigenvectors by Frame's method¹⁵ which is applicable to both symmetric and nonsymmetric matrices. The computed eigenvalues and normalized eigenvectors are presented in Table IV. Since 36 electrons were involved in the calculation and 27 energy levels were computed, 9 of these levels are empty. Hence, the highest occupied level becomes a doubly occupied a_g orbital at an energy of -11.65 eV, and the ground electronic state of Ni(DTAA)₂ is 1A_g . The lowest unoccupied level is a b_{1g} orbital at an energy of -9.47 eV. The assignment of these two energy levels indicated that the molecular orbitals are predominantly metal in character. The first MO is approximately 69% $3d_{x^2-y^2}$ and the second, about 62% $3d_{xy}$. An energy level diagram of the most important levels in Ni(DTAA)₂ is shown in Table V. The sequence of levels proceeding to higher energy is as expected: L(σ) bonding, L(π) bonding, metal d orbitals, and L(π^*) antibonding. The energy separation, $4a_g \rightarrow 3b_{1g}$, or in effect, $3d_{x^2-y^2} \rightarrow 3d_{xy}$, has been labeled Δ_1 .

Since the coordinate system adopted in these calculations is rotated by 45° from the system used in square-planar tetrahalides and other similar compounds, the splitting parameter,¹⁶ Δ_1 , is the reverse of the one-electron transition for the latter complexes.

(14) R. S. Mulliken, *J. Chem. Phys.*, **23**, 1841 (1955).

(15) (a) J. S. Frame, *Bull. Amer. Math. Soc.*, **55**, 1045 (1949); (b) H. E. Fettes, *Quart. Appl. Math.*, **8**, 206 (1950); (c) P. S. Dwyer, "Linear Computations," John Wiley & Sons, New York, N. Y., 1951, pp 225-235.

(16) H. B. Gray and C. J. Ballhausen, *J. Amer. Chem. Soc.*, **85**, 260 (1963).

Table IV. Molecular Orbitals for Ni(DTAA)₂

Eigenvalues	Eigenvectors					
	4s	σ (S)	3d _{z²}	π_h (S)	3d _{x²-y²}	
a_g	39.11	0.72	-0.69	0.11	0.0	0.0
	-12.30	0.24	0.13	-0.96	0.0	0.0
	-16.12	0.31	0.90	0.31	0.0	0.0
	-11.65	0.0	0.0	0.0	0.55	-0.83
	-14.28	0.0	0.0	0.0	0.86	0.52
b_{1g}		3d _{xy}	σ (S)	π_h (S)		
	-9.47	0.79	-0.53	-0.30		
	-13.81	0.14	-0.34	0.93		
	-16.21	0.52	0.83	0.19		
b_{2u}		4p _y	σ (S)	π_h (S)		
	12.54	0.78	-0.60	-0.16		
	-13.69	0.08	-0.03	1.00		
	-14.90	0.05	-1.00	0.02		
b_{3u}		4p _x	σ (S)	π_h (S)		
	12.54	0.78	-0.60	-0.16		
	-13.69	0.08	-0.03	1.00		
	-14.90	0.05	-1.00	0.02		
a_u		π_v (S)	π_v (C)			
	-9.41	0.44	-0.90			
	-16.62	0.96	0.29			
b_{1u}		4p _z	π_v (S)	π_v (C)	π_v (C')	
	0.64	0.59	-0.43	0.53	-0.41	
	-4.77	0.55	-0.03	-0.59	0.60	
	-12.91	0.10	0.36	-0.55	-0.75	
	-16.69	0.07	0.95	0.29	0.04	
b_{2g}		3d _{zz}	π_v (S)	π_v (C)	π_v (C')	
	-7.52	0.08	-0.34	0.76	-0.55	
	-11.78	0.42	-0.33	0.37	0.76	
	-12.51	0.92	-0.02	-0.29	-0.28	
	-16.71	0.15	0.95	0.28	0.02	
b_{3g}		3d _{yz}	π_v (S)	π_v (C)		
	-9.31	0.16	-0.45	0.88		
	-12.43	0.98	-0.10	-0.20		
	-16.71	0.15	0.95	0.28		

Table V. Predominant Energy Levels in Ni(DTAA)₂

	4b _{2g}	L(π^*)
	3b _{3g}	L(π^*)
	2a _u	L(π^*)
	3b _{1g}	3d _{xy}
↑ Energy	4a _g	3d _{x²-y²}
	3b _{2g}	3d _{zz}
	3a _g	3d _{g²}
	2b _{3g}	3d _{yz}
	2b _{2g}	3d _{zz}
	2b _{1u}	L(π)
	2b _{2u} , 2b _{3u}	L(π)
	2b _{1g}	L(π)
	2a _g	L(π)
	1b _{2u} , 1b _{3u}	L(σ)

Results and Discussion

In the Ni(DTAA)₂ spectrum shown in Figure 3 there are six band maxima which are sufficiently intense to be considered allowed transitions. Identical spectra were obtained in a number of solvents including strongly coordinating solvents such as pyridine. The same behavior was observed for the Pd(II) and Pt(II) chelates of dithioacetylacetonate. This suggests axial perturbation by solvent molecules is at a minimum for these complexes and confirms that the first d-d transition involves

Table VI. Electronic Spectrum of Ni(DTAA)₂

Observed maxima, cm ⁻¹	Calculated energy, cm ⁻¹	Log ϵ	Assignment
14,890 (sh)	17,580	2.52	$^1A_g \rightarrow ^1B_{1g}$ ($4a_g \rightarrow 3b_{1g}$)
18,120	18,630	3.45	$^1A_g \rightarrow ^1B_{3g}$ ($3b_{2g} \rightarrow 3b_{1g}$)
18,120	19,120	3.45	$^1A_g \rightarrow ^1B_{2u}$ ($3b_{2g} \rightarrow 2a_u$)
25,150 (sh)	24,360	3.62	$^1A_g \rightarrow ^1B_{3u}$ ($2b_{3g} \rightarrow 2a_u$)
29,670	29,040	4.33	$^1A_g \rightarrow ^1B_{2u}$ ($2b_{1u} \rightarrow 3b_{3g}$)
35,460 (sh)	34,040	4.59	$^1A_g \rightarrow ^1B_{2u}, ^1B_{3u}$ ($2b_{2u}, 2b_{3u} \rightarrow 3b_{1g}$)
36,500	35,490	4.66	$^1A_g \rightarrow ^1B_{1u}$ ($2b_{1g} \rightarrow 2a_u$)
41,150	43,800	4.23	$^1A_g \rightarrow ^1B_{2u}, ^1B_{3u}$ ($1b_{2u}, 1b_{3u} \rightarrow 3b_{1g}$)

Table VII. Electronic Spectra of M(DTAA)₂ Chelates

Transition	Ni(DTAA) ₂	Pd(DTAA) ₂	Pt(DTAA) ₂
d-d			
$^1A_g \rightarrow ^3B_{1g}$ ($x^2 - y^2 \rightarrow xy$)			
$^1A_{1g} \rightarrow ^1B_{1g}$ ($x^2 - y^2 \rightarrow xy$)	14,890 (2.52)	18,120 (2.65)	18,180 (3.45)
$^1A_g \rightarrow ^3B_{3g}$ ($xz \rightarrow xy$)			
$^1A_g \rightarrow ^1B_{3g}$ ($xz \rightarrow xy$)	18,120 (3.45)	19,840 (3.25)	17,480 (3.57)
M \rightarrow L charge transfer			
$^1A_{1g} \rightarrow ^1B_{2u}$ ($xz \rightarrow L(\pi^*)$)	18,120 (3.45)	19,840 (3.25)	17,480 (3.57)
$^1A_g \rightarrow ^1B_{3u}$ ($yz \rightarrow L(\pi^*)$)	25,510 (3.62)	20,490 (3.20)	28,000 (3.90)
L \rightarrow M charge transfer			
$^1A_{1g} \rightarrow ^1B_{2u}, ^1B_{3u}$ ($L(\pi) \rightarrow xy$)	35,460 (4.59)	33,440 (4.11)	35,710 (4.12)
$^1A_g \rightarrow ^1B_{2u}, ^1B_{3u}$ ($L(\sigma) \rightarrow xy$)	41,150 (4.23)	46,300 (4.08)	41,840 (4.52)
L \rightarrow L*			
$^1A_g \rightarrow ^1B_{2u}$	29,670 (4.33)	29,330 (3.82)	29,940 (4.01)
$^1A_g \rightarrow ^1B_{1u}$	36,500 (4.66)	39,530 (4.53)	38,170 (4.28)

d orbitals in the plane of the molecule. The weak shoulder near 14,900 cm⁻¹ was assigned to this parity-forbidden, $^1A_g \rightarrow ^1B_{1g}$ transition. The remaining parity- and spin-forbidden d-d transitions, $^1A_g \rightarrow ^1B_{3g}$, $^3B_{1g}$, and $^3B_{3g}$, were too weak to be observed and have been masked by the proximity of a $^1A_g \rightarrow ^1B_{2u}$, M \rightarrow L(π^*) charge-transfer band near 18,000 cm⁻¹. Charge-transfer bands of the L(π) \rightarrow M type have been found to be separated by about 10,000 cm⁻¹ in other metal complexes. Assigned bands which fit this description are those close to 35,000 cm⁻¹, a L(π) \rightarrow 3d_{xy} transition, and near 41,000 cm⁻¹, a L(σ) \rightarrow 3d_{xy} transition, both of which have the detailed assignment, $^1A_g \rightarrow ^1B_{2u}, ^1B_{3u}$. Bands located near 30,000 cm⁻¹ and 37,000 cm⁻¹ were assigned to transitions mainly on the ligand, L(π) \rightarrow L(π^*), and in this case, $^1A_g \rightarrow ^1B_{2u}$ and $^1B_{1u}$, respectively. The remaining band near 25,000 cm⁻¹ is a M \rightarrow L(π^*) transition, $^1A_g \rightarrow ^1B_{3u}$. M \rightarrow L(π^*) and L(π) \rightarrow M transitions of the type, $^1A_g \rightarrow ^1A_u$, which are orbitally forbidden, would undoubtedly be eclipsed by the more intense allowed transitions described. The assigned transitions for the nickel chelate are summarized in Table VI. Good agreement between observed and calculated band maxima was obtained.

The spectral assignments for Pd(II) and Pt(II) dithioacetylacetonates with the results for Ni(II) as a blueprint, are given in Table VII. Each chelate exhibits a weak band assigned to the first spin-allowed d-d transition, two intense bands at \sim 35,000 cm⁻¹ and \sim 42,000 cm⁻¹ assigned to allowed L(π) \rightarrow M charge-transfer

transitions, two intense bands near 30,000 and 37,000 cm⁻¹ assigned to L(π) \rightarrow L(π^*) transitions, and two moderately intense bands close to 18,000 and 25,000 cm⁻¹ which arise from M \rightarrow L(π^*) charge-transfer transitions.

The electronic spectrum¹⁷ of Co(DTAA)₂ has been recorded previously. The energy level scheme of Ni-(DTAA)₂ was used as a guide for assigning the absorption bands in the spectrum of paramagnetic d⁷ Co(II) dithioacetylacetonate. The occupation of the molecular orbitals, $\dots(3b_{2g})^2(4a_g)^1(3b_{1g})^0\dots$, produced a 2A_g ground electronic state for Co(DTAA)₂. In addition to the bands that have appeared in the d⁸ system, a number of other bands arise from the cobalt complex. The low-energy d-d transitions, $2b_{3g} \rightarrow 4a_g$ and $2b_{2g} \rightarrow 4a_g$, appear at 6750 cm⁻¹ since the $4a_g$ molecular orbital

is now singly occupied. Two additional L(π) \rightarrow M transitions, $2b_{1u} \rightarrow 4a_g$ and $2b_{1u}, 2b_{3u} \rightarrow 4a_g$, appear at 10,870 and 17,500 cm⁻¹, respectively. Another L(σ) \rightarrow M transition, $1b_{2u}, 1b_{3u} \rightarrow 4a_g$, appears near 28,000 cm⁻¹. The remaining bands have the same assignment as those in the d⁸ metal chelates of dithioacetylacetonate. The spectral assignments for Co(DTAA)₂ are summarized in Table VIII.

Although metal chelates of 2,4-pentanedithione have been postulated to possess properties similar to metal dithienes,¹⁸ the present analysis shows that the electronic structure of metal dithioacetylacetonates can be explained in the conventional way as predicted previously.¹⁹ The very intense band in the near-infrared region for neutral dithienes⁴ of Ni, Pd, and Pt and their monoanions² is absent in the spectra of Ni, Pd, and Pt dithioacetylacetonates. Consistent with the spectroscopic observations, the MO calculations reveal no low-lying empty molecular orbitals in Ni(DTAA)₂. Further, the electronic ground state of Ni(DTAA)₂ is determined by an orbital based mainly on the metal in contrast to the π -delocalized ground state proposed for metal dithienes. The presence of a very small energy difference between the highest occupied and lowest unoccupied π molecular orbitals in metal dithienes has been cited as the basis for the semiconducting proper-

(17) R. L. Martin and I. M. Stewart, *Nature*, 210, 522 (1966).(18) J. A. McCleverty, *Progr. Inorg. Chem.*, 10, 49 (1968).(19) G. N. Schrauzer, *Transition Metal Chem.*, 4, 299 (1968); *Acc. counts Chem. Res.*, 2, 72 (1969).

Table VIII. Electronic Spectrum of Co(DTAA)₂

Observed maxima, cm ⁻¹	Log ε	Assignment
6750	1.30	² A _g → ² B _{2g} (2b _{3g} → 4a _g , yz → x ² - y ²)
		² A _g → ² B _{2g} (2b _{2g} → 4a _g , xz → x ² - y ²)
10,870	1.48	² A _g → ² B _{1u} (2b _{1u} → 4a _g , L(π) → x ² - y ²)
17,500	3.60	² A _g → ² B _{2u} , ² B _{3u} (2b _{2u} , 2b _{3u} → 4a _g , L(π) → x ² - y ²)
		² A _g → ² B _{1g} (4a _g → 3b _{1g} , x ² - y ² → xy)
		² A _g → ² B _{3g} (3b _{2g} → 3b _{1g} , xz → xy)
21,600	3.51	² A _g → ² B _{2u} (3b _{2g} → 2a _u , xz → L(π*))
~24,000	3.70	² A _g → ² B _{3u} (2b _{3g} → 2a _u , yz → L(π*))
~28,000	4.18	² A _g → ² B _{2u} , B _{3u} (1b _{2u} , 1b _{3u} → 4a _g , L(σ) → x ² - y ²)
29,400	4.15	² A _g → ² B _{2u} (2b _{1u} → 3b _{3g} , L(π) → L(π*))
36,600	4.45	² A _g → ² B _{2u} , ² B _{3u} (2b _{2u} , 2b _{3u} → 3b _{1g} , L(π) → xy)
40,100	4.30	² A _g → ² B _{1u} (2b _{1g} → 2a _u , L(π) → L(π*))
44,600	4.48	² A _g → ² B _{2u} , ² B _{3u} (1b _{2u} , 1b _{3u} → 3b _{1g} , L(σ) → xy)

ties and high electron affinity of metal dithienes.²⁰ The MO results for Ni(DTAA)₂ suggests that metal dithioacetylacetonates do not possess the above-mentioned characteristics. Furthermore, tris chelates of dithioacetylacetonates²¹ would be expected to possess octahedral symmetry rather than the trigonal-prismatic geometry of tris(dithienes).

If reasonable values for the Slater-Condon interelectron repulsion parameters,²² F_2 and F_4 , are assumed, the corrected splitting parameter, Δ_1 , derived from the first spin-allowed d-d transition, increased in the expected order Ni < Pd < Pt. A correction factor of 2800 cm⁻¹ for Ni²⁺ gave a Δ_1 value of 17,690 cm⁻¹ for Ni(DTAA)₂ and placed the dithioacetylacetonate anion in the spectrochemical series of sulfur donors³ as follows: maleonitriledithiolate (14,490) < diethyl dithiophosphate

(17,300) < dithioacetylacetonate (17,690) < ethyl xanthate (18,300) < diethyl dithiocarbamate (18,600) < 2,3-dimercaptopropanol anion (19,000) < dithiomalonate (20,200) < dithiooxalate (20,500). The order of ligand-field strengths appeared unaffected by molecular geometry since no important trend existed among the four-, five-, and six-membered chelate rings. A correction factor²² ($F_2 = 10F_4 = 600$ cm⁻¹) of 2100 cm⁻¹ for Pd²⁺ produced the following sequence for Pd(II) planar complexes:³ maleonitriledithiolate (17,800) < dithioacetylacetonate (20,220) < diethyl dithiophosphate (23,900) < diethyl dithiocarbamate (24,300) < dithiooxalate (28,100). The order is identical with the series for planar Ni(II) complexes except for the position of diethyl dithiophosphate.

Acknowledgment. The authors thank the National Research Council of Canada for financial support of this work.

(20) E. J. Rosa and G. N. Schrauzer, *J. Phys. Chem.*, **73**, 3132 (1969).

(21) G. A. Heath and R. L. Martin, *Chem. Commun.*, 951 (1969).

(22) H. B. Gray and C. R. Hare, *Inorg. Chem.*, **1**, 363 (1962).